A simple model of oesophageal peristalsis using cellular automata

Kevin R. Haylett†, Patrica Vales§ and Rory F. McCloy

† Medical Engineering
§ GI Investigation Unit
University Department of Surgery
Manchester Royal Infirmary

Keywords: Oesophagus, model, peristalsis, cellular automata, finite element analysis

Address for correspondence:

Dr K. R. Haylett, C.Eng,MIET, FAGIP

Medical Engineering
Manchester Royal Infirmary
Oxford Road
Manchester
M13 9WL

Email: kevin.haylett@cmmc.nhs.uk

Keywords: oesophagus, esophagus, model, peristalsis, cellular automata.

Abstract

The oesophagus is a highly dynamic adaptive organ with a complex physiology. It has a complex physiology including an inner circular and outer longitudinal layer of muscle divided by a neural network, the myenteric plexus. Oesophageal dysfunction has been widely implicated as a cause of gastro-oesophageal reflux disease and non-cardiac chest pain. Although modern instrumentation systems have begun to elucidate the complex nature and dynamics of oesophageal function, muscle function, co-ordination and excitation is poorly understood. A simple generalised model of excitation based upon cellular automata is developed in order to understand the processes that may be occurring in the creation and control of oesophageal peristalsis. This simple model simulates a wave of excitation within a constrained tube using the known properties of excitation and peristalsis. The model simulates the wave of excitation responsible for primary and secondary peristalsis and for tertiary waves. The model also enables investigation of changes in refractory times, regions of dysfunction and activation levels.

1. INTRODUCTION

Our ultimate goal in developing a model is the prediction of future events given a set of initial conditions. The first aim of simulating enteric activity is to develop a coherent understanding of the processes that may be occurring within the motility of the gut. Secondly, to understand the processes that may be leading to disorders and disease. Thirdly, these models may then be used to assist in the development of treatments, in the form of surgical or pharmaceutical therapies.

If we are to contemplate electrically stimulating the gut or developing artificial sphincters such as prosthetic ano-rectal sphincters [1] and new surgical techniques, it is essential that we not only understand the system, but also can reliably predict the outcome of any intervention. The aim of this investigation was to develop a simple model of the

excitation of the oesophagus based upon the available information with a view to linking this excitation to the mechanical activity of the striated and smooth muscle that provide the forces to clear the oesophagus.

1.1 Modelling enteric activity

Modelling of electrical activity of the gut has previously focussed on the use of relaxation oscillators [2]-[4]. These models have been applied to biological rhythms since Van der Pol [5]. The use of these models was based on in vitro experiments, showing the lower gut to have a three dimensional array of electrical oscillators that are coupled in a cylindrical manner. These were lumped models that did not take into account individual neurons. Models of single neurones have developed from the model proposed by Hodgkin and Huxley [6]. These equations, which include terms representing the rates of K+ and Na+ ion exchange, and simplified versions, using the modified Van der Pol equations, sometimes called the FitzHugh-Nagumo [7][8][9] have been shown to be reproduce a great many qualitative characteristics of the neuronal action potential [10].

There has been some debate over which of these methods will be most successful [11] in simulating the complex system innervating the gut. It is has been suggested that both relaxation and core conductor models will provide the best approach to further understanding the gut at both a macroscopic and microscopic level [12]. However, these models do not easily lend them selves to the modelling of excitation and mechanical activity in the oesophagus. In the following sections we briefly examine some recent methods that have been used to model the oesophagus and review the rational for using a simple cellular automata model.

1.2 Mechanical models of the oesophagus

The simulation of Li and co-workers [13] involved treating the oesophagus as a simple distensible tube of finite length with peristalsis modelled as a sinusoidal based travelling wave. The model was formulated using the Navier / Stokes equation for a peristaltic wave,

using the lubrication theory, which neglects bolus inertia and assumes a gentle radial wall curvature. This model did not take into account the role of the longitudinal muscle, its excitable nature or its active control. However, the results of the model did compare visually with those from previous fluoromanometry studies [14]. The model did demonstrate that treating the oesophagus as a simple distensible tube and peristalsis as a simple single-wave process could not explain manometry observations occurring within the transition zone of the oesophagus. It concluded, based on the model developed, that the result of a low-pressure wave detected at the aortic notch was not consistent with a single peristaltic wave and could only be explained by a second wave restarting after the aortic notch. It was hypothesized that the clinical observations may result from the different types of muscle, striated and smooth, which begin to differentiate in this region.

1.3 Modular models

Another approach to modelling intestinal peristalsis has used a modular approach based on the components of the enteric nervous system. In the simplest approach [15], circular muscle was considered as a series of overlapping modules. Each module contained all the elements of the enteric system. A control algorithm was written, with the functional elements for each module being represented by a single composite element. As a possible mechanism of connection and weighting of these components it was demonstrated that these simplified functional elements were capable of generating a wave function. However, this model did not take into account the longitudinal muscle or refractory nature of the peristaltic reflex.

A simple Boolean model of the relationship between longitudinal and circular muscle has also been presented [16]. This model based on clinical observations, treats the two layers as discrete units and suggests that opening of the lower oesophageal sphincter is dependent on these units operating in the correct sequence.

1.4 Physiological model of enteric activity

A more physiologically based approach to modelling small bowel activity, taking into account enteric neurophysiology using modified Huxley equations and compartmental pharmaco-kinetic synaptic models, was carried out by Miftakhov and co-workers. This approach developed earlier models of the excitatory (cholinergic) [17][18] and inhibitory (adrenergic) [19][18] neurons into a planar enteric network [20] (also see [41] and [42]).

A similar approach using overlapping electromechanically connected functional units, 'loci', was used to simulated motility patterns of the small bowel [21]. Although the authors suggest the technique offers a good basis for modelling the enteric nervous system and myogenic activity of the small bowel, successfully recreating observed patterns of neural excitation; they recognize the difficulties of the approach. These difficulties include a lack of information of the detailed neuronal structure, with both primary afferent neurons and secondary sensory neurons having yet to be definitely identified. Their model is uniform, idealized and null dimensional, i.e. the complex shape and layout of the neurons are ignored. The model, which is necessarily complex, requires 97 variables and constants; if the spatial complexity of GI morphology and neurophysiology were included, this approach would ultimately lead to a multi-dimensional model, with further constants and variables requiring quantification. However, the techniques to measure all the necessary variables, such as integrative properties of neurons and individual synaptic properties, have yet to be developed. The authors conclude that their model simulates some experimentally observed activity and needs further development and comparison with experimental and theoretical data. Although this approach may yield results at the microscopic scale, extending the model to larger scale involves a considerable reliance on the initial assumptions.

In modelling oesophageal function there are many possible approaches being. For example Figure 1 shows a simple model of excitation, developed during this study, based upon a feedback based control system. It is quite possible that there is some underlying system that operates in this manner i.e. the system aims for a target value, and following sensory feedback relaxes. It is known that the de-innervated oesophagus is capable of still

creating a peristaltic wave. It is quite imaginable that such a control process is involved in the generation of the peristaltic wave with feedback components operating between the muscles of the oesophagus and the myenteric plexus. However, such models are speculative based upon our understanding of control theory in engineering systems and may be extremely difficult to apply to the oesophagus, in anything more than a highly simplistic model as shown in Figure 1.

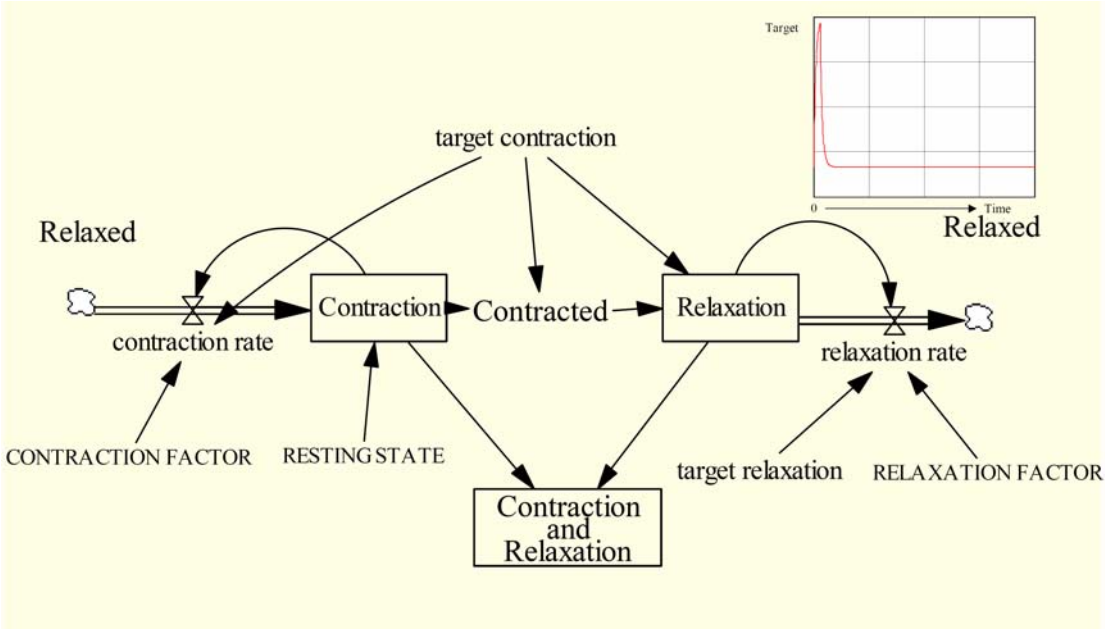

Figure 1 Control model of peristalsis. This figure shows a simple example of a highly speculative, control model of excitation. Inset shows the results of a simple numerical simulation (simulated using 4 variable Runge-Kutta integration using a typical modelling program (Ventana-Systems-Inc., 1996)).

Although peristalsis is possible in the de-innervated oesophagus [22], it is known that there is additional control from the swallowing centre, which has been shown to produce sequential excitation along the length of the oesophagus in a second level control system. This is also modified by sensory neurones that are part of the process. Ideally a generalised model of the oesophagus should have the characteristics that excitation will i) generate the pattern of excitation intrinsically and ii) be capable of modification of this process via higher order control processes.

1.5 Simulating oesophageal excitation using cellular automata.

In this study we have tried to base the simulation on the known large scale characteristics of the oesophagus, with a view to exploring oesophageal function, including that of the longitudinal muscle. Investigations of oesophageal peristalsis have demonstrated that the observed peristaltic wave has the basic properties of excitable media i.e. material that has the basic properties of an activation level, an excitation level, an equilibrium or un-excited level and a refractory period [23][24]. The mechanism of the refractory period is unclear although the study by Meyer and co-workers suggested that it resulted from both the refractory nature of the muscle component and neural inhibition from a preceding swallow. This conclusion was drawn from the observation that in investigating coupled swallows the second swallow was reduced in amplitude. However, this result may also be due to the contraction of the longitudinal muscle of the second swallow, adding vector force to the first swallow and effectively reducing the effect of circular muscle contraction. To confirm this hypothesis further investigation and modelling of the forces resulting from both longitudinal and circular components would be required.

It is likely that the refractory period plays a role in reducing the risk of aspiration. A succession of peristaltic waves would increase the probability, proportional to the number and the time interval between swallows, of the lumen appearing closed (as the contraction would present a barrier). Fluids or solids propelled by pharyngeal swallowing would then be prevented from entering the proximal oesophagus. A refractory period allows the oesophagus above the contraction to act as a secondary chamber that can be filled, while the distal oesophagus is being cleared, thereby reducing the risk of aspiration. To some extent this was demonstrated in mechanical models of swallowing which showed the pressures present at the aortic notch are not consistent with a continuous propagating swallow i.e. even for normal swallows this region is acting as a primary chamber. It is often the case that during radiology the barium can be seen to fill this region, before flowing or being cleared distally.

Excitable tissue, such as that of a single neurone, can be modelled by standard techniques using continuous partial differential equations (PDEs) representing a homogenous media with an excitable mechanism. These PDEs are generally solved using standard finite-difference methods. Although models combining several elements can be used to simulate a network of neurones, as the number of neurones included is increased, the model becomes increasingly speculative.

With the advent of digital computing, recent techniques have included the discrete method of cellular automata (CA) models. A CA model is based upon an array of identically programmed automata or "cells" which interact with one another. The arrays usually form a 1,2 or 3 dimensional set of nodes. Often, for the purpose of modelling, the cells are arranged in a simple rectangle although other arrangements such as a honeycomb can be used. The essential features of a cellular automaton are its *state*, *neighbourhood* and *program*. The *state* is a variable that takes a different value for each cell. The *state* can be either a number or property. The *neighbourhood* is the set of cells with which any individual cell interacts. In a grid these are normally the cells physically closest to the cell in question. The *program* is the set of rules that defines how the cells state changes in response to its current state, and that of its neighbours in a discrete time step (t).

In the classical Greenberg-Hastings CA model of excitable media each cell can be considered as a simple one-dimensional model, which can then be expanded to two and three-dimensions. Using the simplest possible model for excitable media the cell can be in three distinct states that are functions of media variables. For instance a nerve cell can be in a state of excitation, refractoriness or equilibrium (relaxed phase), with the excitatory and refractory periods being functions of cell transport mechanisms. Although early cellular automata models have been used to model biological processes, continuous partial differential equation models have dominated recent theory of spatial temporal organisation in excitable media. Early CA models used a simple nearest neighbour algorithm and lacked many essential features [25]. These included the change in wave velocity resulting from the shape of the wavefront and dispersion, where the speed of the wavefront depends on the extent of media

recovery in front of the wave. Also, the speed of planar wave propagation in a homogeneous isotropic medium should be the same in all directions. Many early CA models exhibited gross anisotropies in speed relative to the underlying grid. Recent studies have shown that these effects can be improved by extending the region of excitation and using a process of weighting excited cells in that region until a threshold is reached [26][27].

The functional weighting of neural systems and networks is not trivial. Any model of more than a few neurones in the enteric neural system would be quite speculative. The mechanism of excitation within the oesophagus is far more complex than that of a single nerve or single region of muscle. It has a highly complex control system influenced by a wide range of external physical factors. In this study we have used a CA model for the generalised excitation of the enteric nervous system. This model allows an investigation into the properties of a homogonous region of excitable media within the constraints of a tube. It allows the effect of changes in the size of the region of excitability to be investigated (this is analogous to the region neurones can span). Also, it allows the effects of regions of increased, decreased and failed excitability to be investigated.

The implicit variables of the CA model include a definition of the neighbourhood, it size and its properties, including the refractory and excitation periods together with its program, which incorporates the properties of the identified region. Investigations of the enteric nervous system of the intestine have shown that motor neurones innervating the circular and longitudinal muscles have short dendrites and a single axon of up to 1.6cm. Inter neurones project long distances of up to 3.6cm (these increase to 6.8cm towards the lower bowel) [28]. The velocity of the propagating circular segment corresponding to the lumen obliterating peristaltic wave (smooth muscle) is 3-4 cm/S and the refractory period is between 4 and 8 seconds [23]. The region of contraction seen during video-fluoroscopy is typically several centimetres corresponding to the length of the excitatory neurones. These values give an order of scale to be investigated in the developed model.

Some work has been started on understanding how the various types of neurones are connected to create a region of excitation but early work has been speculative. In our case we began by considering the simple excitation-refractory model previously described

METHODS

2. Simulating excitation

The developed generalised model of excitation (GME) of the oesophagus uses the classical CA model of excitable media with an extended Moore neighbourhood as described by Gerhardt [26]. The GME is represented by a spatially distributed excitable medium, using a rectilinear lattice of cells (**L**) obeying the same local rules. The rule for spatial spread of excitation is that an unexcited cell will become excited in the next discrete time step if it is sufficiently recovered and if a sufficient number of its neighbours are already in an excited state (see equations 1 to 7). The extended Moore neighbourhood $\boldsymbol{N^m}$ is a square of cells within a rectangular region of "radius" $\mathbf{r}^x$ and $\mathbf{r}^y$ centred on a given cell (i,j) i.e.

$\boldsymbol{N^m}_{(i,j)}$ is the neighbourhood in lattice **L** of all cells (x,y), see Figure 2.

where $| x-i | <= \mathbf{r}^x$ and $| y-j | <= \mathbf{r}^y$ } (Equ-1)

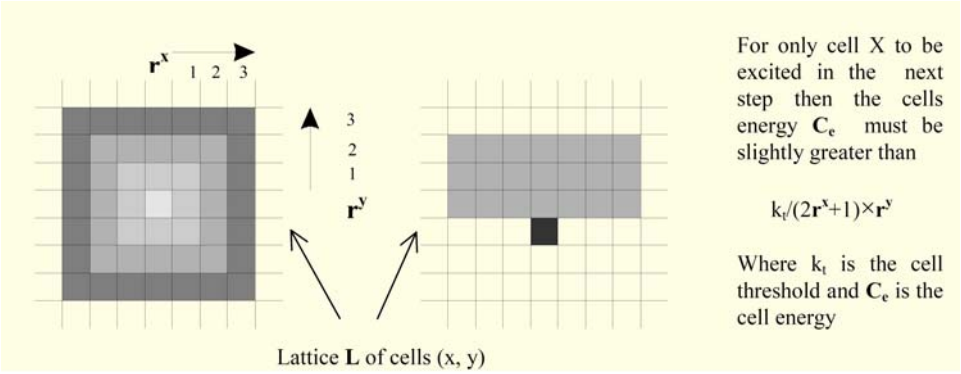

Figure 2 Extended Moore's radius. a) Shows a lattice L of cells (x, y) with extended Moore's neighbourhood of different sizes. b) Shows the region of cells requiring excitation to linearly propagate a cell in a single time step.

Each cell **C** has an energy variable $\mathbf{C_e}$, which is 0 when unexcited and takes a value $\boldsymbol{k_e}$ when excited. Each cell also has a variable $\mathbf{C_r}$ indicating the cell's state of recovery. If $\boldsymbol{E^m}$ is the total energy in the neighbourhood $\boldsymbol{N^m}$ and $\boldsymbol{k_t}$ is the cell's threshold value, $\boldsymbol{k_r}$ is the recovery period, which includes the period of excitation $\boldsymbol{k_{et}}$ and the refractory period $\boldsymbol{k_r}$ - $\boldsymbol{k_{et}}$. Then the rules for the next step $\mathbf{C}_{(n+1)}$ in the CA are:

(1) If the cell is unexcited and the total energy $\boldsymbol{E^m}$ is greater than the threshold $\boldsymbol{k_t}$ the cell becomes excited.

$\mathbf{C}_{\mathbf{e}(n+1)} = \boldsymbol{k_e}$ when $\mathbf{C_r} = 0$ and $\boldsymbol{E^m} > k_t$ (2)

(2) If the cell is already excited it will remain excited with energy $\mathbf{C_e}$ equal $\boldsymbol{k_e}$, until it enters into its refractory state when its energy $\mathbf{C_e}$ will be set to 0. The recovery variable $\mathbf{C_r}$ will be incremented until it is greater than the recovery period $\boldsymbol{k_r}$ in which case it will become unexcited and $\mathbf{C_r}$ will be reset to 0.

$\mathbf{C}_{\mathbf{e}(n+1)} = 0$ when $\mathbf{C_r} > 0$ $\boldsymbol{k_{et}}$ and $\mathbf{C_r} < \boldsymbol{k_r}$ (3)

$\mathbf{C}_{\mathbf{r}(n+1)} = \mathbf{C_r}+1$ when $\mathbf{C_r} < \boldsymbol{k_r}$ (4)

$\mathbf{C}_{\mathbf{r}(n+1)} = 0$ when $\mathbf{C_r} > \boldsymbol{k_r}$ (5)

Using an extended Moore radius has two advantages in the case of modelling oesophageal excitation. Firstly, Gehardt and co-workers have shown that CA with an extended Moore neighbourhood better approximate the effects of curvature associated with travelling waves in excitable media [26]. Secondly, we can use a fine lattice for a more accurate representation and adjust the region to reflect the range of the inter-neurones. It is likely that the energising effect of the inter-neurones are related to a number of factors including their type, position and firing rates relative to any given cell i.e. cells further away may have less effect than cell's nearby. However, little detail is known about the *myenteric plexus* and we have therefore assumed that all cells in the neighbourhood $\boldsymbol{N^m}$ contribute equally and have a similar $\mathbf{C_e}$.

In modelling the mechanism of excitation the dividing myenteric layer was considered as a 2 dimensional region of uniformly excitable media, where the left and right vertical edges closed to form a three dimensional tube. This layer was modelled as a 20 × 1.3cm area of continuous uniformly excitable media. The circumference at the *myenteric plexus* was 1.3cm taking into account a muscle wall diameter of approximately 0.1cm at the *myenteric plexus* and a non-excitable catheter width 0.3cm placed in the central lumen. The width and height of each cell in the CA was 0.1cm. A local propagation velocity of 4cm/S was assumed, with each time step (δt) corresponding to a time period of 0.025S. The study of multiple swallows by Ask and Tibbling [23] showed that only 18% of swallows repeated every 4 seconds and 75% of swallows repeated every 8S were successfully propagated in the distal section. These periods were used to model the waveform, which was considered excitatory during the period of contraction. The results are presented for a 4S waveform i.e. excitatory for 1.5S for the contraction period and refractory for a further 2.5S.

The effect of neighbourhood size on the propagation was investigated using a vertical radius $\mathbf{r}^{y}$ of between 0.5cm and 3.6cm reflecting the region of influence of both the descending and ascending neurones. A horizontal radius $\mathbf{r}^{x}$ of between 0.2cm and 0.9cm was used reflecting lateral interconnections.

2.1 Visualising muscle forces

To assist in visualising the progress of the wave a simple colour map was used. This colour map was based on an approximation of the cellular tensions generated during a normal swallow. In the erect position a fluid bolus travels ahead of the peristaltic stripping wave due to the effect of gravity. It is assumed that the axial component is the principle force generated. The longitudinal contraction may affect the overall force. However, evidence suggests that longitudinal contraction travels ahead of the circular contraction and that the axial force is principally derived from the contraction of the local circular muscle contracting in a uniform manner providing the ‘squeeze’. This enables an estimation of the tension for each of the cells. The intra-luminal pressure P is given by Laplace’s Law P= T / r where r is the radius of

the lumen and t the wall tension. If we assume that each cell contributes equally to the overall wall tension then for a measured intra-luminal pressure P, the cell tension is given by Tc = (P×r) / Nc, where Tc is the cellular tension and Nc is the number of cells. The cellular tensions applied to the circular muscle can therefore be calculated from the intra-luminal forces at each point of a typical peristaltic contraction.

A simple linear piecewise approximation was used to model the LCF (local contraction force). The contraction used for the LCF was selected from a non-symptomatic subject by an experienced clinician to represent what was considered clinically normal. The peak height used was 75mmHg with positive gradient of 79 mmHg/S and negative gradient of -53 mmHg/S and baseline of 0 mmHg [29]. It is possible to replace this simple force map with a mathematical function in a more complete model. Although these forces are only mapped here as an aid to visualisation of the wave progress, it may be possible to map them to a mechanical mesh model of the oesophagus.

3. RESULTS

Although generalised CA modelling environments are available, the simulation was carried out using a program specifically designed and developed during this study to model the GME of the oesophagus. The program was developed using Microsoft® Visual Basic 5, This software was designed with an easy to use graphical interface that both displayed the states of the cells and allowed the initialisation of the CA variables (see Figure 3). The developed program performed the following functions:

- Displayed the states of cells.
- Displayed colour map to show cell tensions.
- Allowed dimensions of model and refractory and excitatory periods to be set.
- Computed linear approximation of tension map or read map from file.
- Allowed regions with a random percentage of cells to be set to a given state.
- Allowed size of the Moore's neighbourhood and the cells energy to be set.
- Allowed output of state map and cell tensions of the model for further processing.

• Allowed the model to be set to stop automatically when a given cell had changed to a predefined state.

This program was found to be easy to use and created output files of the results to enable visualisation, using AVS-Express [40]. The results of our CA experiments can be divided into two groups. Firstly, qualitative model properties, which describe the consequences of using a CA model of a GME for the oesophagus and secondly, quantitative results, which illustrate the effects of the numerical algorithm and parameters used. The flexibility of the model presented allows modifications of these parameters to be investigated. The GME was investigated by both increasing and decreasing the excitability of the CA and by changing the size of the region of excitation.

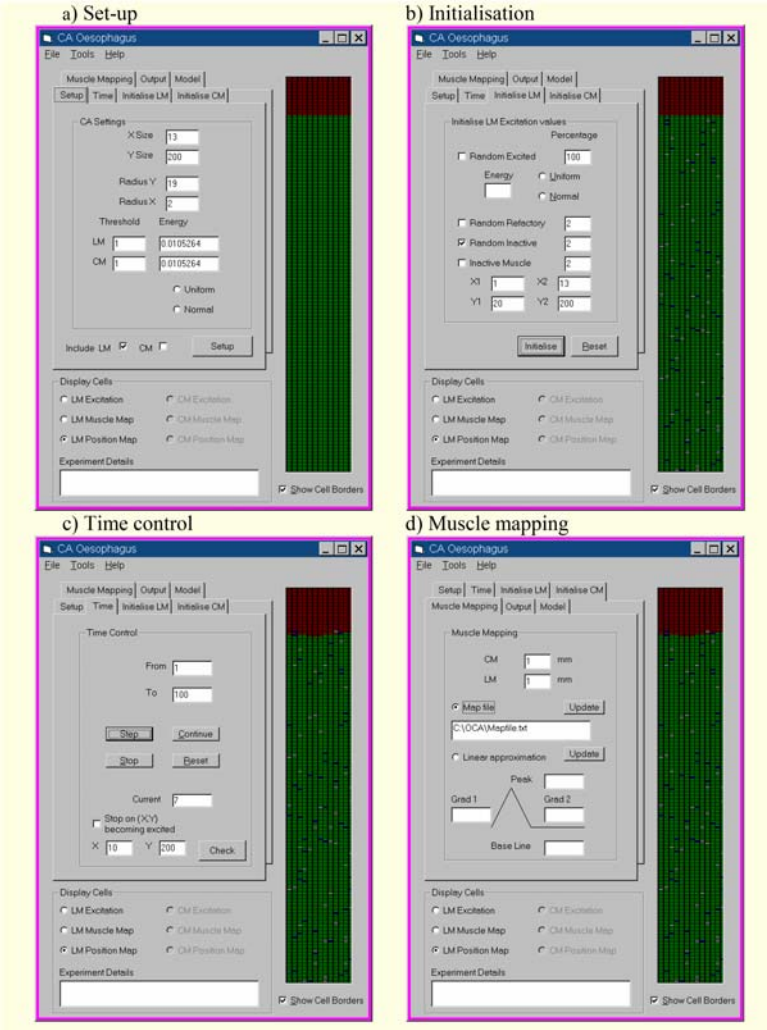

Figure 3 The CA Program. This figure shows the GUI for the program developed to simulate the generalised model of excitation for the oesophagus. a) The tabbed dialog interface used to set up the CA. b) The dialog used to set up the area of differing functionality. c) The time control dialog and d) the dialog used for mapping the CA to a contraction function.

3.1 Qualitative GME features

Initialisation of a propagating wave – For a cell to become excited the critical values are the size of the neighbourhood (Nm), the excitability of the cell and the total excitation energy (Em) generated within this region. A travelling wavefront will only be initiated when Em > kt i.e. a relatively large distributed region requires stimulation in a single time step to start a propagating wavefront. The initial conditions for the CA are for Ce to be set to a value to produce a propagating wave with a unit velocity by making Ce slightly greater than kt /(2rx +1)×ry. The results indicated that, given the constraints of the model, a large neighbourhood will fail to propagate a wave in the presence of even a small region of dysfunctional media. The results also showed that the smaller the region Nm the greater the ability of the system to propagate a wavefront around any regions of dysfunction. This is explored numerically in the next section.

Regions of high and low excitability – The effect of increased excitability or sensitivity is to increase the velocity of the travelling wave. The overall effect on the wave velocity is dependent on the number of cells with a high excitability or high sensitivity. The effect of decreased excitability is to stop or slow the wavefront down. A wavefront will be able to pass small regions of low or zero excitability as long as Em > kt for the surrounding cells, enabling the wave of excitation to travel around the unexcitable region. However, if Em <= kt, a critical value, the wavefront will collapse over a region smaller than the extended Moore's Neighbourhood.

High-speed propagating wavefront – Figure 4 shows an example of a high speed propagating wavefront. The model has been initially seeded with both an initial region excited to start the propagating wavefront and an additional 5% of excited and 2% inactive cells have also been

included ahead of the initialised wavefront. The effect of the additional excitation outweighs the inactive cells and substantially increases the overall rate of propagation.

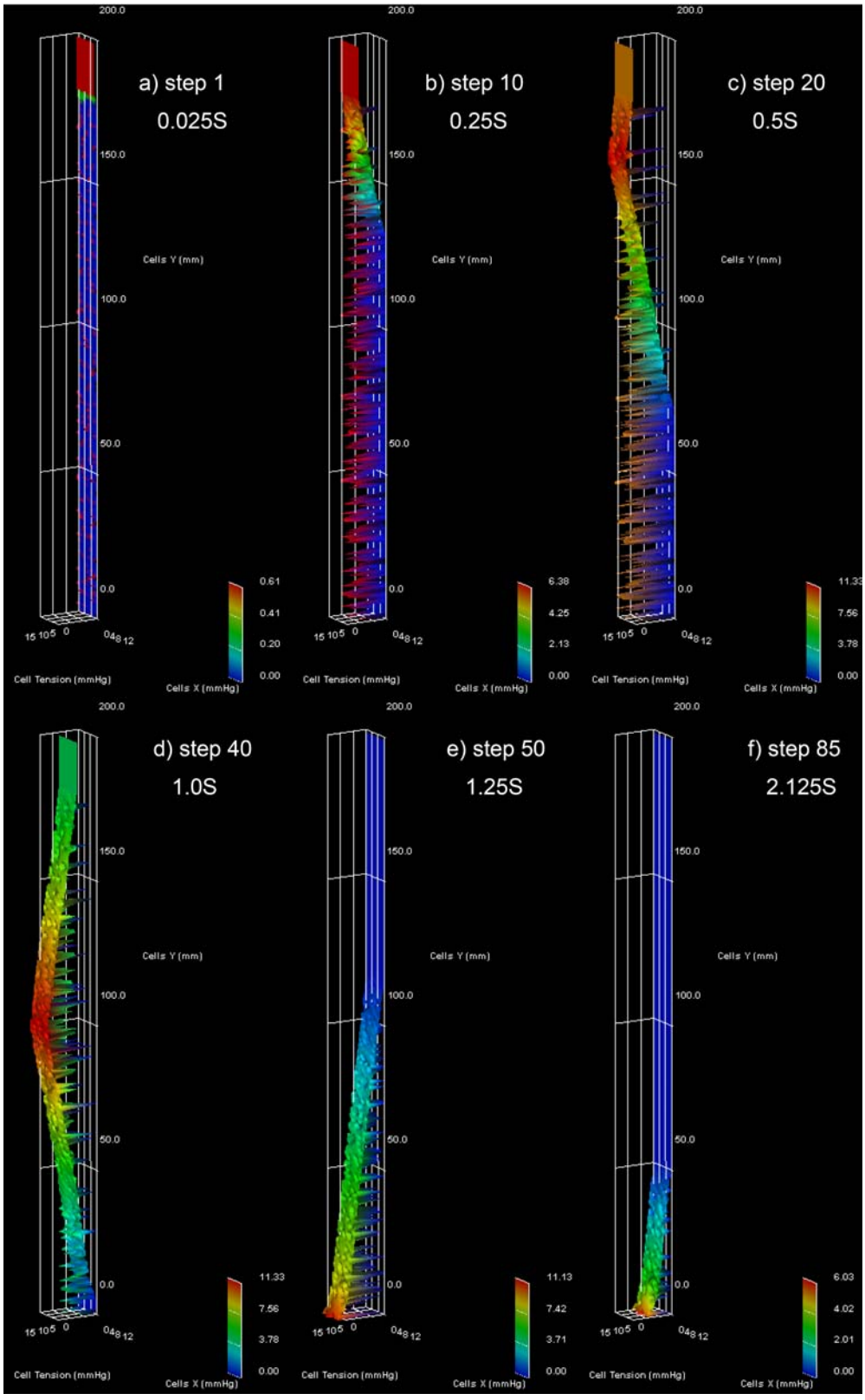

Figure 4 High speed propagating wavefront. This figure shows successful propagation of a travelling wavefront following sufficient initial excitation. The initial conditions include a random number of excited (5%) and inactive (2%) cells (rx = 0.2cm and ry = 1.9cm).

Hyper-excited wavefront – Figure 5 shows an example of a wavefront where the model is seeded with additional 40% randomly excited cells (and 5% inactive) ahead of the initialised propagating wave. The net effect is that there is little discernible wavefront and the whole of the model becomes excited all at once i.e. equivalent to a true simultaneous contraction.

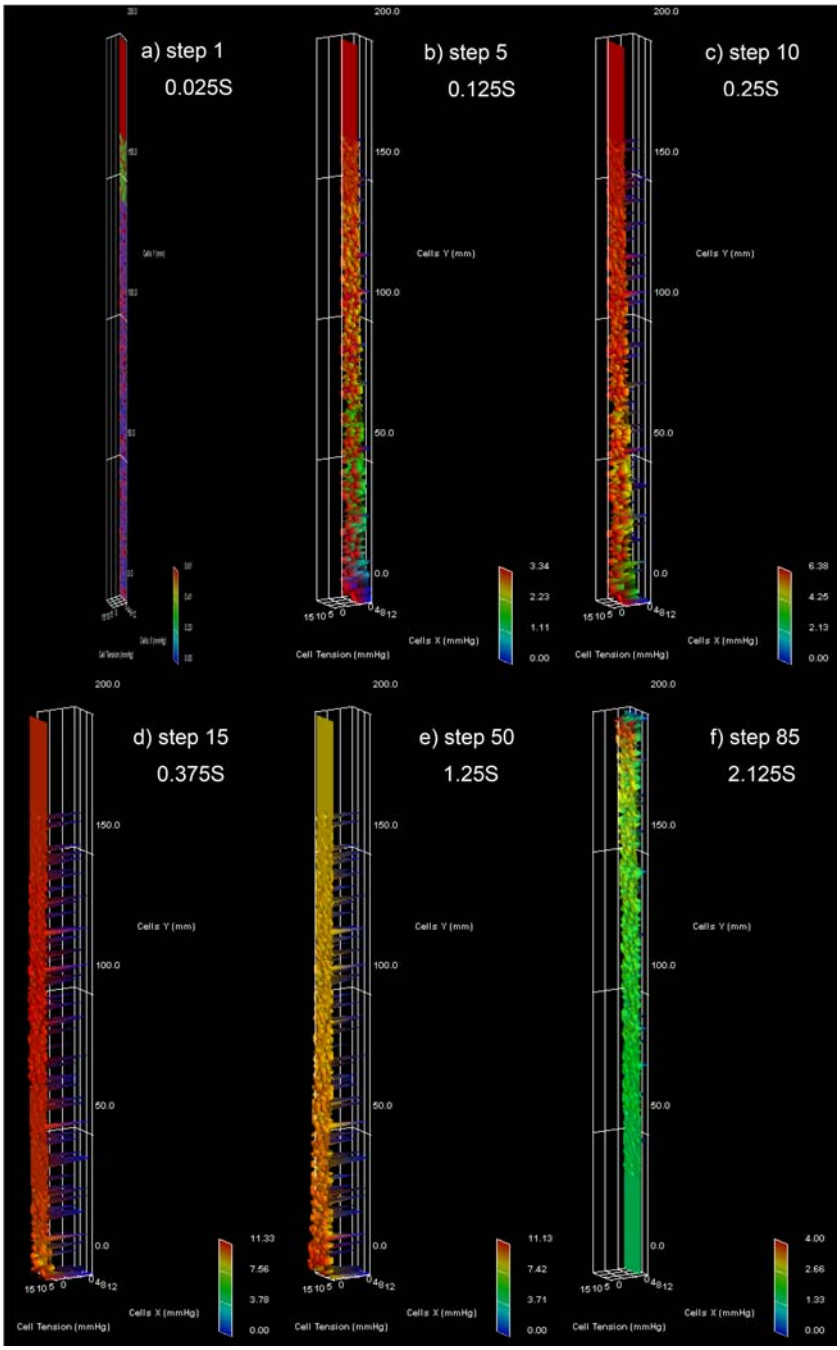

Figure 5 Hyper-excited (simultaneous) wavefront. This figure shows simulation of a travelling wave with a large number of randomly excited (40%) and inactive (5%) cells resulting in a simultaneous (hyper-excited) wavefront (rx = 0.9cm and ry = 3.5cm).

Failed wavefront – Figure 6 shows an example of wavefront failure. In this example the model was seeded with the both the initialised wavefront and 3% active and 1% inactive cells. The overall effect is swallow failure. Although the swallow starts to propagate the cells activated ahead of the wavefront enter their refractory period, these refractory cells contribute to the overall number of inactive cells to such an extent that the wavefront collapses.

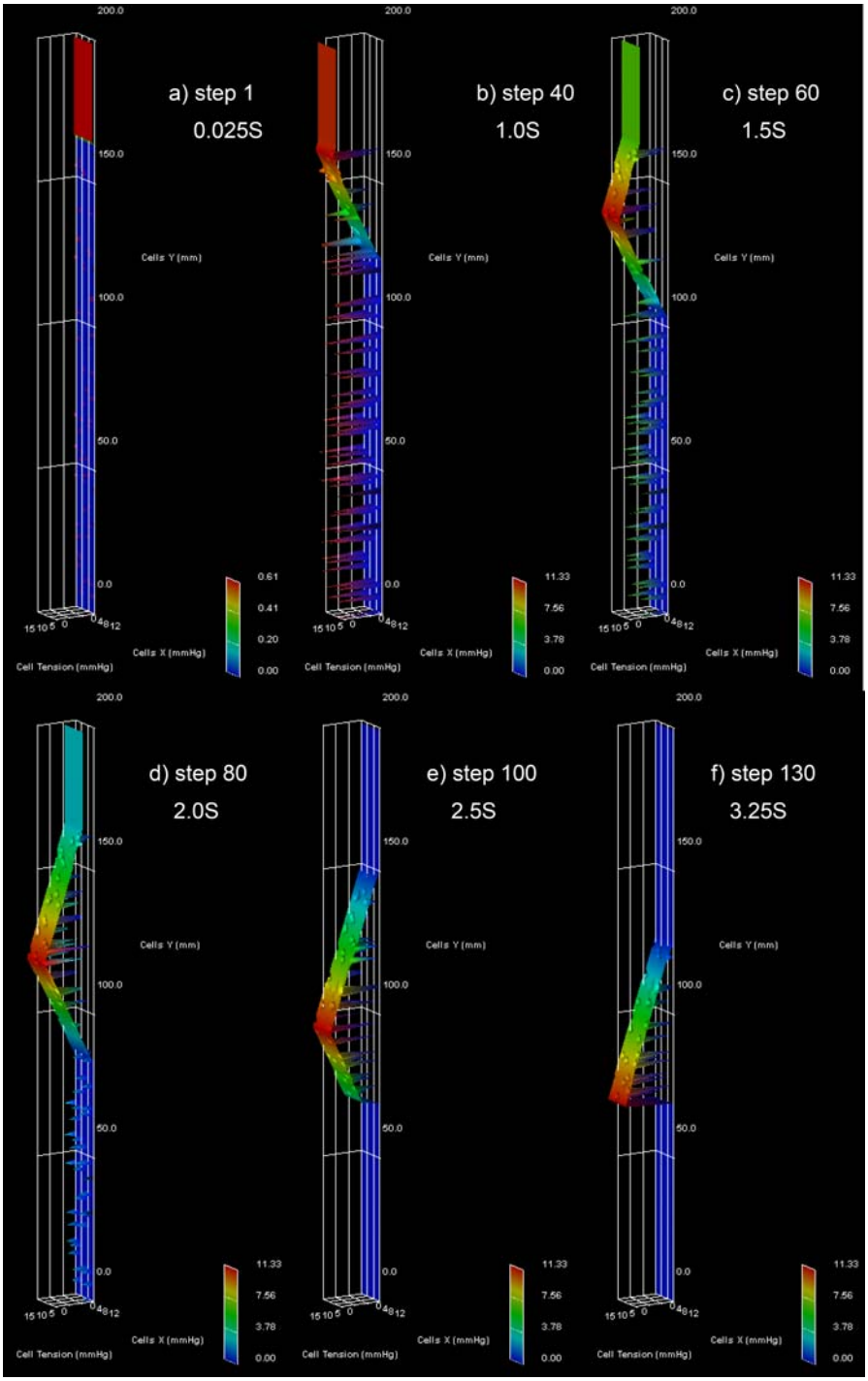

Figure 6 Failed wavefront. This figure shows that cells excited ahead of the wavefront at the beginning of the swallow (1% inactive, 3% active) may become refractory. These may then interfere with the wavefront causing it to fail (rx = 0.9cm and ry = 3.5cm).

Failure at the LOS - Of special interest is the region corresponding to the interface of the distal oesophagus and the LOS, where the wave finally completes its progress. In the model used, the Moore's neighbourhood is considered to surround any given cell in all directions. Cells in this region have their Moore's neighbourhood effectively reduced, as there is no more excitable media. This means that the effects of cells that have failed, or are unable to supply excitation energy due to being in a refractory state, are substantially increased. It is not possible for the wave to overtake these failed regions. Although the wave has passed along the oesophagus with a similar level of non-contributory cells up to this region, the wave fails to reach the end of the CA model. This is demonstrated in Figure 7 where an initiated wave is shown to fail at the end of the model. The initial conditions include a proximal region, maximally excited to ensure an initial propagation of the wavefront with the remaining 5% of the cells randomly selected to refractory. The effects of increased and decreased excitability are investigated numerically in the next section.

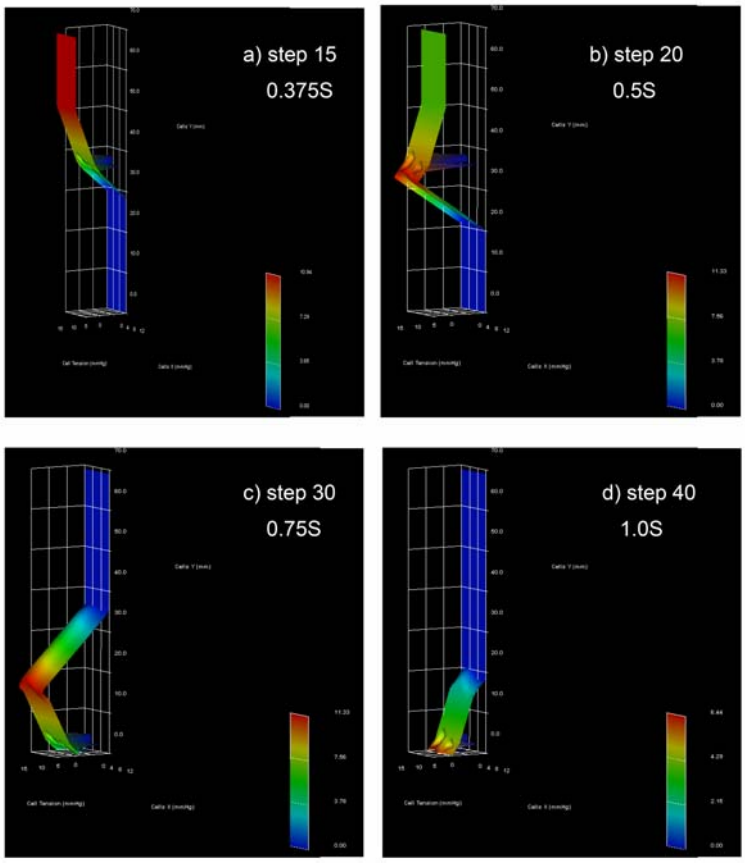

Figure 7 Failure at the LOS. Although the travelling wave can circumvent a region of inactive cells, it takes a number of steps of the model for the wavefront to fully recover. If the same region occurs just before the end of the model active cells may fail to become excited. (rx = 0.2cm and ry = 1.9cm).

No direction encoding – In common with most models of excitable media stimulating a region of size Nm or greater at some midpoint within the CA with an energy Em > kt and with all other cells in an unexcited state, will result in a both an ascending and descending travelling wave.

Wavefront annihilation - Due to the constraints imposed by a tube of excitatory media, descending and ascending wavefronts will meet and result in annihilation of wavefronts. If the initialised waves are sufficiently close, the final wave may appear to have originated from a single more distributed source. If there is only manometric evidence of contraction peaks confusion over the true sequence of muscle activation could occur. For example, a simultaneous contraction, as measured by coincident peaks at different points in the oesophagus, could result from either a high-speed wave of excitation caused by high excitability or from two separate wave process starting at different points within the oesophagus (see Figure 8).

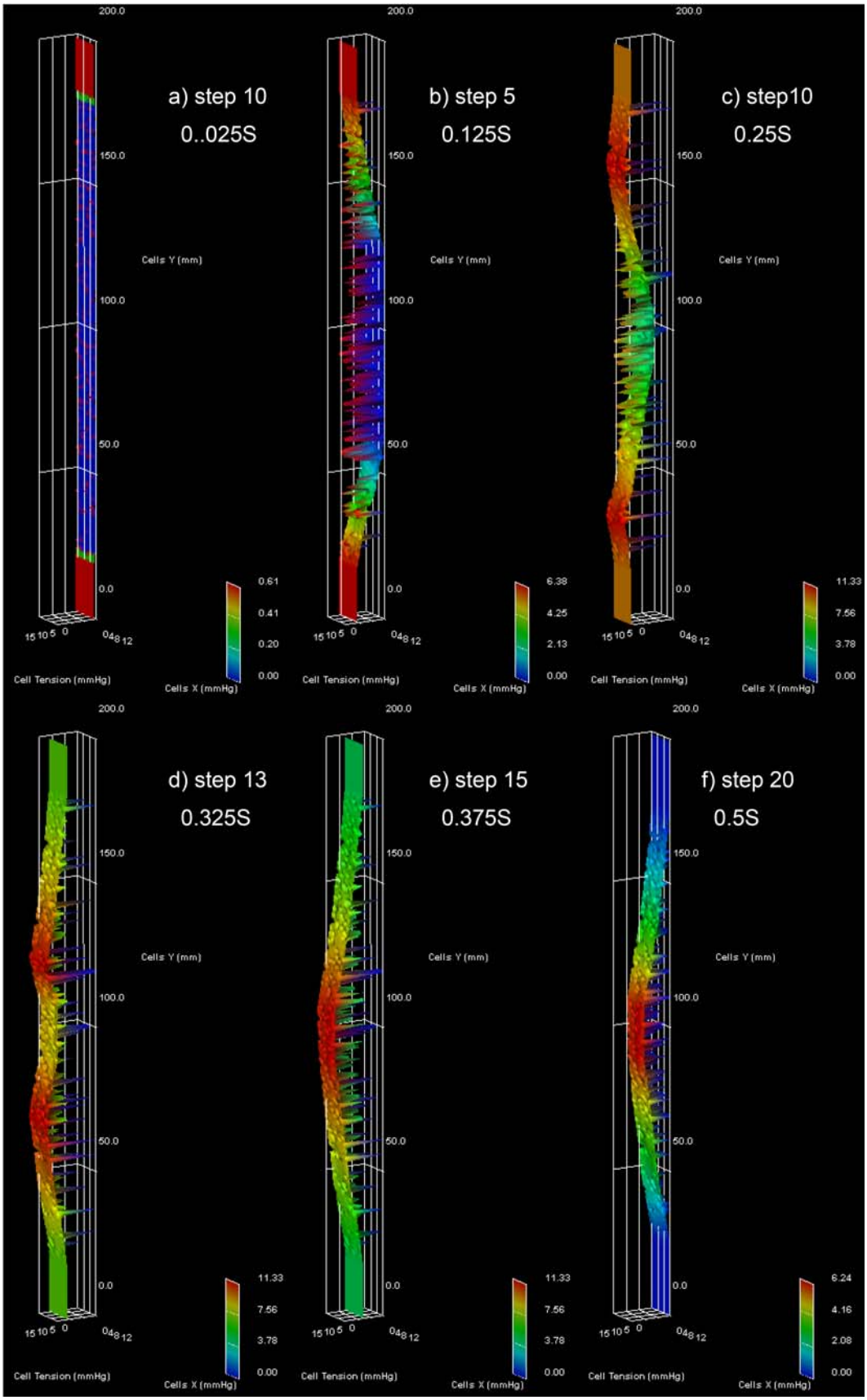

Figure 8 Wavefront annihilation. This figure shows the effect of wavefront annihilation resulting from ascending and descending waves of excitation. In this example the model was also initialised randomly with 2% inactive and 10% active cells (rx = 0.2cm and ry = 1.9cm)

Spiral waves - Excitatory media modelled using CA predicts that under certain condition spiral waveforms of excitation and unstable random activity can be generated [27][28]. These conditions would generally result from an excitatory and refractory period on a considerably reduced scale, in comparison to the propagating peristaltic wave. These spiral waves have been widely explored and implicated in models of cardiac fibrillation [29][30]. However, the phenomena seen in the oesophagus, where there appears to be a spiral like contraction, during radiology and endoscopy, may be related to the spiral waves seen in CA models of excitability. This could provide an interesting area for further research with CA models.

3.2 Quantitative GME features

Increasing excitability - To simulate increased excitability it is possible to introduce a number of cells with a lower threshold for excitation, ke, so these will become excited more easily. Alternatively cells with a higher than normal energy of excitation, Ce, causing other cells to be more excited, could also be introduced. However, for simplicity, we modified the CAs initial condition to include, firstly, a uniformly excited region at the proximal end to ensure a propagating wave front. Secondly, a number of excited cells were randomly distributed through the rest of the CA i.e. cells which have been over excited at initiation of the swallow in an uncoordinated manner. The model was run ten times and the average velocity for the face of the wave front to travel to the end of the CA computed. Both the effect of increasing the percentage of over excited cells and the effect of changing the size of the region Nr were investigated. The results are shown in Figure 9.

It can be seen that for all Nr computed, an addition of only 20% excited cells ahead of the wave front will cause an increase in velocity from 4cm/S to between 14cm/S (rx=2,ry=9) and 26cm/s (rx=9,ry=36) i.e. increasing the size of Nr increases the effect of additional excitation ahead of the propagating wavefront.

Smaller regions give rise to more complex patterns of excitation. Areas ahead of the initial wave can become sufficiently excited to initiate new independent centres of excitation. It is of note, that if the speed of the wavefront is not sufficient to traverse the length of the CA

before the randomly excited cells enter their refractory period, these cells will have effectively become unexcited and will not contribute an energy term Ce. This may influence successful propagation of the wave. The extent of this effect is examined in the next section.

Decreasing excitability - Again simulation of decreased activity could be achieved by either increasing the threshold, ke, or decreasing cell energy, Ce, of cells within the CA. Decreased excitability was investigated by modifying the initial conditions of the CA to include a defined region of cells with zero excitability, simulating a region of dysfunction. The ability of the CA to sustain a propagating wave was examined in relationship to the size of the Moore's neighbourhood Nr (Table 1). Any unexcited cell that has these inactive cells in its neighbourhood may fail to be come excited if the total energy available from the whole neighbourhood does not exceed the threshold. The excitatory period can also come into play. If an earlier excited cell returns to its non contributory (refractory) state and is still in the neighbourhood of the advancing wave front then it acts as another failed cell and may stop the progress of a wave front.

Table 1 shows that the smaller the neighbourhood size the greater the region of failed cells that may be circumvented. The wave front can effectively go around the failed area. If the neighbourhood is large then due to the constraints of the model the region of failed excitability cannot be bypassed.

3.3 Relationship to clinical observations

Swallow initialisation - This simple model of excitation has many characteristics, which correspond to clinical observations of the oesophagus. Successful swallows are defined by a manometrically observed pressure contraction and radiologically by a lumen clearing stripping wave. The oesophagus can be divided into three regions, the upper striated zone, the transition zone and the lower smooth muscle zone. It is known that the striated muscle of the upper oesophagus has additional connections to the swallow centre of the brain. These

connections may explain the fast initialisation in the extended Moore's neighbourhood predicted by the GME.

Disorders involving decreased contractile activity - Clinical examinations may reveal hypotensive manometry with little evidence of a stripping wave. The peristaltic wave is often seen to be reduced in amplitude with the wave collapsing within a distance of a few centimetres. The model presented shows that a small regions of failed or refractory cells ahead of the propagating wavefront will cause it to collapse (see Table 1 and Table 2). The model predicts that the successful propagation of a wavefront might be assisted by additional extrinsic excitation or by a combination of intrinsic and extrinsic inhibitory processes that ensure regions ahead of the wavefront are not prematurely excited.

Moore's Neighbourhood N^m	**Maximum region of failed excitability while still propagating wavefront**
$\mathbf{r}^x$ (cm) = 0.2 $\mathbf{r}^y$ (cm) = 0.9 $\mathbf{C_e}$ (Excitation constant) =0.02223	0.1×0.4cm  0.4×0.1cm 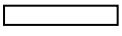 0.2×0.2cm 
$\mathbf{r}^x$ (cm) = 0.2 $\mathbf{r}^y$ (cm) = 1.9 $\mathbf{C_e}$ (Excitation constant) =0.0105264	0.1×0.3cm  0.4×0.1cm 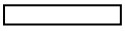
$\mathbf{r}^x$ (cm) = 0.4 $\mathbf{r}^y$ (cm) = 2.9 $\mathbf{C_e}$ (Excitation constant) =0.00384	0.1×0.1cm 
$\mathbf{r}^x$ (cm) = 0.9 $\mathbf{r}^y$ (cm) = 3.5 $\mathbf{C_e}$ (Excitation constant) =0.0015038	Always fails

Table 1 **Decreased excitation.** The effect of neighbourhood size on the ability to propagate beyond regions of failed excitation, excitatory period = 60 (1.5S), refractory period = 100 (2.5S).

Disorders involving increased contractile activity – Clinically many patients present with abnormal motility patterns that are classified as simultaneous. Simultaneous motility patterns are characterised by a contraction at several recording sites with less than 1 second between onset of the observed peak. This may correspond to increases in excitability Ke , Ce or

randomly excited cells ahead of the propagating wave. These changes give rise to an increase in wavefront velocity (see Figure 9).

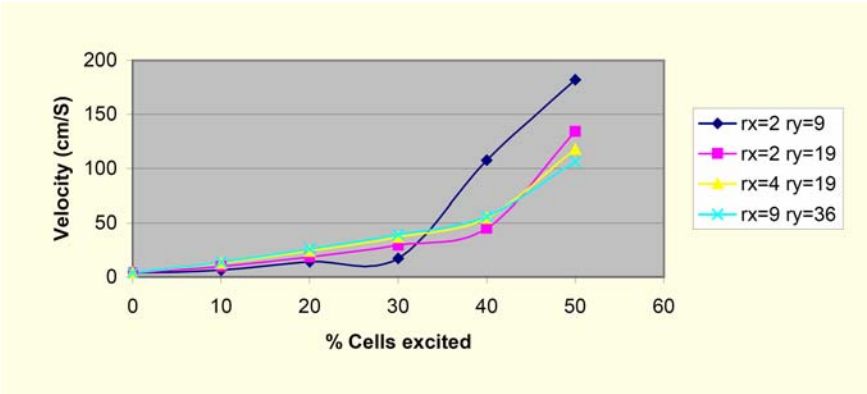

Figure 9 Increasing Excitability. This graph shows the effect of introducing randomly excited cells on the velocity of a wavefront, for various sizes of Moore's Neighbourhood Nm .

Run	**1**	**2**	**3**	**4**	**5**	**6**	**7**	**8**	**9**	**10**
Propagation	**1% Inactive Cells**									
Success/Failure	S	S	S	S	S	S	S	S	S	S
Time to fail or complete (S)	8.68	8.53	8.33	8.95	8.98	8.90	8.43	8.28	9.00	9.03
V(cm/S)	2.24	2.29	2.13	2.13	2.15	2.27	2.31	2.12	2.12	2.24
	1.2% Inactive Cells									
Success/Failure	F	F	S	F	S	F	F	S	F	S
Time to fail or complete (S)	4.13	1.80	10.88	1.18	12.18	1.25	3.98	10.55	4.50	10.58
V(cm/S)	-	-	1.76	-	1.57	-	-	1.81	-	1.81
	!.5% Inactive Cells									
Success/Failure	F	F	F	F	F	F	F	S	S	F
Time to fail or complete (S)	2.18	1.60	1.75	2.38	1.95	2.55	2.13	10.15	10.20	2.33
V(cm/S)	-	-	-	-	-	-	-	1.88	1.87	-
	2% Inactive Cells									
Success/Failure	F	F	F	F	F	S	F	F	F	F
Time to fail or complete (S)	2.15	0.85	0.43	3.08	2.35	10.78	1.28	1.45	1.20	0.85
V(cm/S)	-	-	-	-	-	1.77	-	-	-	-

Table 2 **Decreased excitation.** This table shows the increase in failed propagation with increasing percentages of inactive cells ahead of the wavefront. This data is for a model with N^r with $\mathbf{r}^x$=0.2cm and $\mathbf{r}^y$=1.9cm, excitatory period = 60 (1.5S), refractory period = 100 (2.5S). The table shows that increasing the number of inactive cells also causes a decrease in the wavefronts velocity.

Disorders involving failure at the LOS – Decreased contractile activity and failure of the bolus to be transferred from the oesophagus to the stomach through the LOS is implicated in many oesophageal motility disorders. Extreme failure occurs in the disorder Achalasia, where food or liquid is unable to pass into the stomach. This is characterised by the absence of peristalsis and failure at the LOS. Treatment for this includes balloon dilatation at the LOS and ultimately surgery to release the pressure at the high-pressure zone. Although clinically this disorder is well defined, less advanced forms of this condition are observed and difficult clinical decisions have to be made as to the options available for intervention.

Our evidence from fluoromanometry studies, where the manometry and bolus can be visualised together, shows that good peristalsis at the distal region is important for good clearance into the stomach. During a successful swallow of fluid in the upright position the bolus flows distally through an open lumen under the effect of gravity. The bolus is then held at the LOS until a peristaltic wave pushes it through the LOS. The model presented here demonstrates that this distal region is more sensitive to inactive regions of excitation. This suggests a possible aetiology of disorders involving failure at the LOS i.e. small amounts of damage to the lumen, as seen as oesophagitis due to excessive reflux, may interfere with the mechanism of excitation, following which clearance is less successful, with further damage occurring proximally until finally the peristaltic wave is unable to push the bolus into the stomach.

Direction encoding – The developed model does not have any implicit direction encoding, although the Moore's neighbourhood could be modified to ensure a direction component. This means that the model will simulate both normal and retrograde peristalsis, both of which are observed during radiological studies. The model predicts that sufficient stimulation of a region midway along the oesophagus will initiate both descending and ascending wavefronts. Orvar and co-workers [31] reported strong contractions both distal and proximal to the site of balloon distension. A further more detailed study of distension response has shown that the response varies at different levels of the oesophagus [32]. Williams and co-workers suggest

their results indicate an inhibitive element of control that spans the length of the oesophagus, this may be extrinsic. The model presented here assumes only intrinsic local control in a homogenous excitable mediium. The change in response at different levels observed by Willliams and co-workers may result from either variations in the size of the Moore's neighbourhood, its 'program' or the extrinsic innervation of the oesophagus Additionally, sustained distension has been shown to elicit a specific response with complex activity above the site of distension and inhibition below the site of distension [33]. A detailed analysis of these patterns and the refractory times associated with these phenomena may assist in developing a more physiologically accurate model, which includes a more detailed representation of initialisation.

Tertiary and random activity – Although less common, other observations made during manometry includes tertiary activity. Here a contraction is observed at a single point in the oesophagus. The model presented here suggests that this phenomena may result from i) a localised region of contraction that fails to initiate a propagating wave front or ii) a propagating ascending or descending contraction which fails due to regions of decreased excitation or iii) from annihilation of ascending and descending wavefronts. Multi-peaked contractions associated with diffuse oesophageal spasm can also be observed. CA models of excitation show that spiral waves can develop, however numerical experiments suggest that the local refractory and excitatory times would have to be far less than those modelled here. This suggest that complex patterns may have an element of extrinsic control

Transition zone problems - Initial deglutition involves passing the bolus quickly into the oesophagus. Often this involves several successive swallows where the oesophagus may not have recovered from previous swallows. If the bolus is propelled into a passive oesophagus, primary peristalsis is considered to have failed. After a short recovery period, a swallow finally pushes the bolus through the oesophagus; this initiates a contraction that passes to the distal smooth muscle. It has been extensively reported that there is a critical region of

excitation at the transition zone. Fluoroscopically we see, in some patients presenting with non-specific motility disorders, the failure of the swallow to progress beyond this point. In our model this equates to the neighbourhood Nm being insufficiently excited or to a decrease in sensitivity in the myenteric plexus. The CA model predicts that a region the size of the neighbourhood within the length of the transition zone will require stimulation; if this fails the wave will collapse.

4. DISCUSSION AND CONCLUSIONS

4.1 Model predictors

The success of a model is usually considered in terms of its ability to predict and explain real world observations. It is well known that the vagotomised oesophagus will support oesophageal peristalsis. Additionally higher-level control via extrinsic innervations has been demonstrated including a centralised pattern generator [34]; however, the need for this control has yet to be explained. The nature of local control within the myenteric plexus is also unknown and although many neural components have been identified and early models postulated, these are in their early stages. It has been demonstrated, using simple mathematical models, that connecting neurones into a feedback circuit introduces a delay [35]. With the propagation velocity of a nerve action potential being up to 100m/S and across the surface sarcolemma of a muscle 2-6m/S [36], it is likely that a significant role of the intrinsic neurones is to create or modulate the delay, which results in a much slower propagation velocity of 4cm/S.

The simple CA model of excitation presented here shows that increasing the size of the Moore's neighbourhood Nm increases the effect of regions of cells not contributing an energy term. This in turn increases the probability of the wavefront collapsing. In this model the cells (which in effect represent a small region of the myenteric plexus and not individual neurons) may not contribute because they are either refractory or dysfunctional.

If an area of cells were dysfunctional the only way of ensuring the propagation of the wavefront would be to supply additional energy via functioning cells or via an external

energy source. Under real world conditions a wide variety of conditions of excitation are likely to exist prior to swallow initialisation and many of the nerves that make up a cell may be in a refractory state. For example, if oesophageal content had stimulated a secondary wavefront, distal cells may become refractory interfering with a primary swallow. This suggests a role for the extrinsic higher oesophageal pathways i.e. afferent pathways serve to monitor the current progress of the wavefront and efferent excitatory pathways provide additional stimulation to re-enforce the generation of the peristaltic wave, which would otherwise collapse. Alternatively extrinsic inhibitory pathways may assist in preventing regions ahead of the propagating wavefront from being prematurely excited, as these can cause a high-speed or simultaneous contraction.

This model also predicts a role for the intrinsic inhibitory neurones. It is possible that these act as a feed forward mechanism to ensure that the overall state ahead of the wave front remains unexcited. This would therefore stop any regions from becoming prematurely refractory, and thereby increase the probability of the wave front successfully propagating. It is of note that the model presented could be further developed to include a local inhibitory component into the CA program. This would not require an accurate knowledge of the underlying control system but would enable parameters such as field of influence and level of inhibition to be investigated using the developed model.

4.2 Mapping excitation to muscular activity

The model does not simulate the generation of local muscular forces. It has been developed to examine the global effects of a GME initiating a simplified muscular response. The problem of understanding the generation of muscular forces under the control of the enteric nervous system is ill posed. The nature of the coupling of the myenteric network and its control system is still unclear and has not been addressed here. However, this study has shown that it may be possible to map the excited nodes of the cellular model on to a mesh model of the oesophagus using a local contraction function (LCF). By using a separate CA model for excitation of the longitudinal muscle and circular layer of muscle the effects of a

delay between contractions of these two wave fronts can be investigated and compared with clinical observations. The mesh model can then be solved using the technique of finite elements (see Figure 10). In this technique the forces in the mesh are solved for applied forces or known movements at each element for each discrete time period (t). This allows a dynamic model of the forces and motions within the walls of the oesophagus to be built up. This is not trivial, as the mechanical behaviour of soft tissues is both complex and nonlinear [37]. However, first order estimates are possible and are beginning to be used in biological simulation and modelling [38][20].

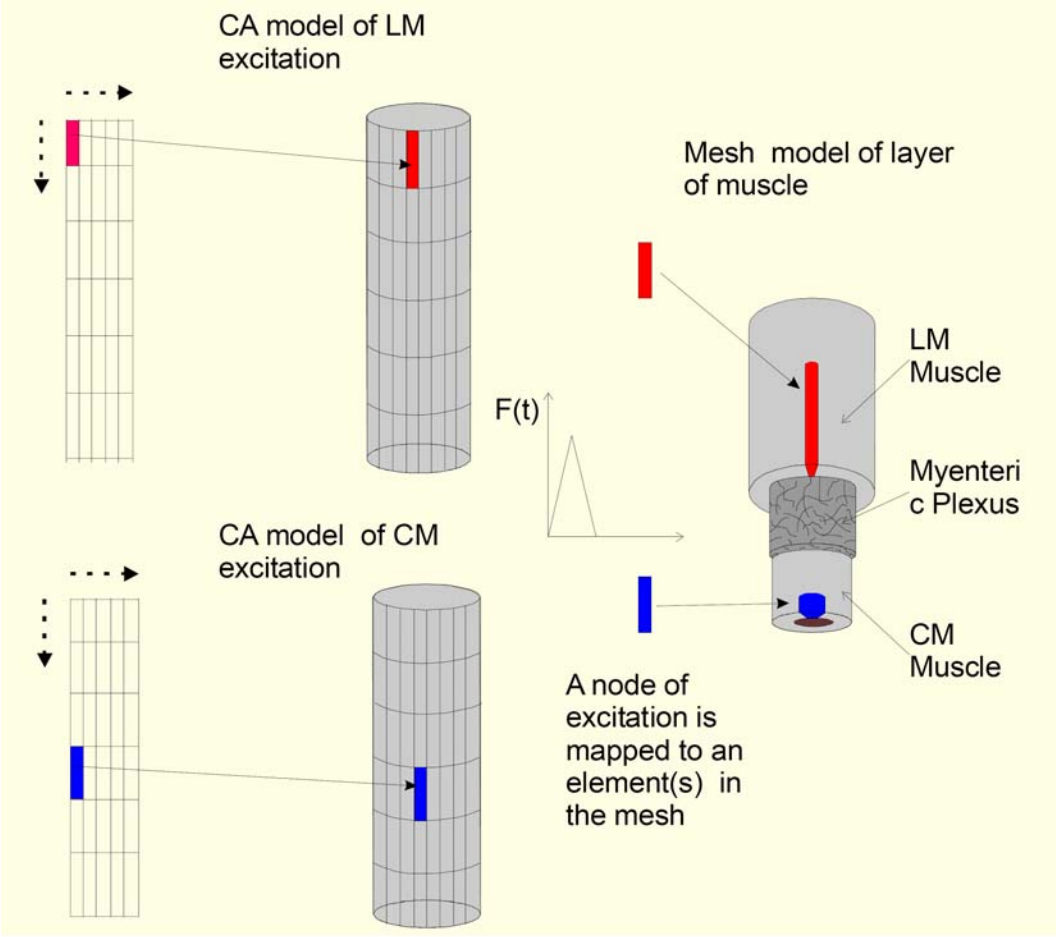

Figure 10 Mapping the CA model to a mechanical mesh. This figure demonstrates how a CA model of excitation can be mapped to a mechanical mesh model of the oesophagus to provide a first order model of the forces that may be occurring during peristalsis.

Oesophageal manometry measures axial forces. Although the principle component of this force is generally assumed to be generated by the circular muscle, the longitudinal shortening has been shown to provide an additional force and to assist in bolus propagation

[39]. Developing this model to include the mechanical forces generated from the circular and longitudinal muscle would enable these effects to be investigated. In particular a more accurate model of the region of the lower oesophageal sphincter, the diaphragm and the stomach is required to allow further investigation of the role of oesophageal shortening on opening of the LOS.

CA methods offer an alternative approach to the classical approach of using partial differential equations for excitable media in the gut. The technique has many possibilities for investigators in that it enables excitation to be linked to the muscular activity and mechanical models of the gut. It may also be extended by the inclusion of pacemaker cells to model the activity of the lower gut and regions where there is no muscle mapping function, simulating regions of muscle atrophy.

Oesophageal dysmotility is widely implicated in gastro-oesophageal reflux disease with symptoms such as heartburn, reflux and non-cardiac chest pain. Therapy is often in terms of disease management with the use of proton pump inhibitors or prokinetic drugs. However, in severe cases of dysmotility, involving failure of food to be passed into the stomach or in excessive reflux resulting in oesophagitis, surgery is carried out. Future work may involve improving the model to reflect the complexity observed during clinical investigations, ideally to produce a virtual oesophagus.

These techniques could also be used to investigate the effects of surgical intervention on peristalsis i.e. by modifying the CA or mesh model to simulate the effect of surgery thus acting as an aid to surgical intervention therapies.

Additionally, the current model could be modified to include a more probabilistic based algorithm to provide a more ‘real’ simulation i.e. the energy levels of excited cells could be based on a probability distribution. The program of the CA could also be developed to take into account any developments in the understanding of the intrinsic innervation of the oesophagus.

Oesophageal modelling is in its infancy and the model presented here is highly simplistic. It is clear that with more complete modelling we could look to the development of

more advanced therapies such as functional electrical stimulation in gastro-oesophageal disorders and the development of artificial sphincters.

In conclusion this study we have used a CA model to emulate the excitable nature of the oesophagus. This model uses the consensus model of excitable media with an extended Moore neighbourhood to reflect the region of inter-neurones influence. This simple GME has the essential features of excitation observed in the oesophagus i.e. it emulates primary, secondary peristalsis and tertiary contractions. Regions of high excitability predict high speed and simultaneous contractions of the oesophagus. Regions of low excitability predict failure of contraction propagation. Both these effects are observed in oesophageal investigations involving motility disorders. The model suggests that the distal region is more susceptible to failed areas of excitability. It also suggests that any proposed method of artificial excitation would have to stimulate a sufficient region to initiate peristalsis. This would require close experimental and more accurate numerical modelling to determine parameters such as current density, area of electrodes and nature of stimulation (number and types of pulses etc.).

This model has not taken into account either the detailed properties, or types of neurones, which create the excitation of the oesophagus. It may be possible to include these as generalised properties, in a more complex model, using additional state variables in a similar manner described by Rhandawa [15]. The process of muscle fibre recruitment and generation of the local muscular forces has not been included in the model; these have been approximated from clinical observations. Again, with further experimental data, it may be possible to include a more complete model of this function. Although currently not including these parameters, the GME and finite element analysis proposed do allow numerical investigation of both the effects of changes in excitability and muscle function and of the mechanical properties of the oesophagus.

Figure 1 Control model of peristalsis. This figure shows a simple example of a highly speculative, control model of excitation. Inset shows the results of a simple numerical simulation (simulated using 4 variable Runge-Kutta integration using a typical modelling program (Ventana-Systems-Inc., 1996)).

Figure 2 Extended Moore's radius. a) Shows a lattice L of cells (x, y) with extended Moore's neighbourhood of different sizes. b) Shows the region of cells requiring excitation to linearly propagate a cell in a single time step.

Figure 3 The CA Program. This figure shows the GUI for the program developed to simulate the generalised model of excitation for the oesophagus. a) The tabbed dialog interface used to set up the CA. b) The dialog used to set up the area of differing functionality. c) The time control dialog and d) the dialog used for mapping the CA to a contraction function.

Figure 4 High speed propagating wavefront. This figure shows successful propagation of a travelling wavefront following sufficient initial excitation. The initial conditions include a random number of excited (5%) and inactive (2%) cells (rx = 0.2cm and ry = 1.9cm).

Figure 5 Hyper-excited (simultaneous) wavefront. This figure shows simulation of a travelling wave with a large number of randomly excited (40%) and inactive (5%) cells resulting in a simultaneous (hyper-excited) wavefront (rx = 0.9cm and ry = 3.5cm).

Figure 6 Failed wavefront. This figure shows that cells excited ahead of the wavefront at the beginning of the swallow (1% inactive, 3% active) may become refractory. These may then interfere with the wavefront causing it to fail (rx = 0.9cm and ry = 3.5cm).

Figure 7 Failure at the LOS. Although the travelling wave can circumvent a region of inactive cells, it takes a number of steps of the model for the wavefront to fully recover. If the same region occurs just before the end of the model active cells may fail to become excited. (rx = 0.2cm and ry = 1.9cm).

Figure 8 Wavefront annihilation. This figure shows the effect of wavefront annihilation resulting from ascending and descending waves of excitation. In this example the model was also initialised randomly with 2% inactive and 10% active cells (rx = 0.2cm and ry = 1.9cm).

Figure 9 Increasing Excitability. This graph shows the effect of introducing randomly excited cells on the velocity of a wavefront, for various sizes of Moore's Neighbourhood Nm .

Figure 10 Mapping the CA model to a mechanical mesh. This figure demonstrates how a CA model of excitation can be mapped to a mechanical mesh model of the oesophagus to provide a first order model of the forces that may be occurring during peristalsis.

REFERENCES

[1] Hajivassiliou, C.A., Carter, K.B., and Finlay, I.G. 1997. Biomechanical evaluation of an artificial anal sphincter prosthesis. Journal of Medical Engineering and Technology 21 (3-4):89-95.

[2] Bardakjian B. L., and Sarna, S.K.. 1981. Mathematical investigation of populations of coupled synthesized relaxation oscillators representing biological rhythms. IEEE Transactions on Biomedical Engineering 28 (1):10-15.

[3] Bardakjian, B.L., and Sarna, S.K. 1980. A computer model of human colonic electrical control activity. IEEE Transactions on Biomedical Engineering 27 (4):193-202.

[4] Sarna, S.K., Daniel, E. E., and Kingmar, Y. J.,. 1972. Simulation of the electric-control activity of the stomach by an array of relaxation oscillators. Digestive Deseases 17 (4): 299-310.

[5] Van der Pol, B. 1940. Biological Rhythms Considered as Relaxation Oscillators. Acta Med. Scand. Suppl. 108:76-88.

[6] Hodgkin, A.L., and Huxley, A.F. 1952. A quantitative description of membrane current and its application to conduction and excitation in nerve. Journal of Physiology 116:500-544.

[7] Murray, J.D. 1989. Hodgkin-Huxley theory of nerve membranes: FitzHugh-Nagumo model. In Mathematical Biology. New York, USA: Springer.

[8] FitzHugh, R. 1969. Mathematical models of excitation and propagation in nerve and muscle. In Biological Engineering, edited by H. P. Schwan. New York, USA: McGraw-Hill.

[9] Nagumo, J., Arimoto, S., and Yoshizawa, S. 1962. An active pulse transmission line simulating nerve axon. Proc. IRE 50:2061-2070.

[10] Zykov, V.S. 1987b. Mathematical description of processes of generation and propagation of electrical excitation in biological excitable tissues. In Simulation of wave processes in excitable media, edited by A. T. Winfree. Manchester, UK: Manchester University Press.

[11] Publicover, N.G., and Sanders, K.M. 1989. Are relaxation oscillators an appropriate model of gastrointestinal electrical activity. American Journal of Physiology 256 (Gastrointest. Liver Physiol. 19): G265-274.

[13] Li, M., Brasseur, J., and Dodds, W. 1994. Analyses of normal and abnormal esophageal transport using computer simulations. American Journal of Physiology 266 (4 Pt 1):G525-543.

[14] Kahrilas, P.J., Dodds, W.J., and Hogan, W.J.. 1988. Effect of peristaltic dysfunction on esophageal volume clearance. Gastroenterology 94 (1):73-80.

[15] Randhawa, S., Nazeran, H., Mayo, R., Brookes, S.H.J., and Costa, M. 1996. The enteric neural network and three dimensional modelling of intestinal peristalsis. Australasian Physical and Engineering Sciences in Medicine 19 (3):168-171.

[16] Stiennon, O.A. 1995a. A boolean model of the oesophagus. In The longitudinal muscle in oesophageal disease. Madison, USA: WRS Press.

[17] Miftakhov, R.N., and Wingate, D.L. 1993. Mathematical modelling of the enteric nervous network. II: Facilitation and inhibition of the cholinergic transmission. Journal of Biomedical Engineering 15 (4):311-318.

[18] Miftakhov, R.N., and Wingate, D.L. 1994b. Mathematical modelling of the enteric nervous network. 1: Cholinergic neuron. Medical Engineering and Physics 16 (1):67-73.

[19] Miftakhov, R.N., and Wingate, D.L. 1994c. Modelling of the enteric nervous network: 3. Adrenergic neuron. Medical Engineering and Physics 16 (6):450-457.

[20] Miftakhov, R.N., and Wingate, D.L. 1994a. Biomechanics of small bowel motility. Medical Engineering and Physics 16 (5):406-415.

[21] Miftakhov, R.N., Abdusheva, G.R., and Christensen, J. 1999. Numerical simulation of motility patterns of the small bowel. 1. Formulation of a mathematical model. Journal of Theoretical Biology 197 (1):89-112.

[22] Ren, J., Massey, B., Dodds, W., Kern, M., Brasseur, J., Shaker, R., Harrington, S., Hogan, W., and Arndorfer, R. 1993. Determinants of intrabolus pressure during esophageal peristaltic bolus transport. American Journal of Physiology 264 (3 Pt 1):G407-413.

[23]Ask, P., and Tibbling, L.. 1980. Effect of time interval between swallows on esophageal peristalsis. American Journal of Physiology 238 (Gastrointest. Liver Physiol., 1):G485-G490.

[24] Mayer-Kress, G., and Hübler, A. 1989. Time evolution of local complexity measures and aperiodic perturbations of nonlinear dynamical systems. In Quantitative measures of complex dynamical systems, edited by N. B. Abraham, A. M. Albano, T. Passamante and P. Rapp. New York, USA: Plenum.

[25]Weimar, J., Tyson, J.J., and Watson, L.T. 1992. Third generation cellular automaton for modeling excitable media. Physica D 55:328-339.

[26]Gerhardt, M., Schuster, H., and Tyson, J.J. 1990a. A cellular automation model of excitable media including the effects of curvature and dispersion. Science 247:1563-1566.

[27] Gerhardt, M., Schuster, H., and Tyson, J.J. 1990b. A cellular automaton model of excitable media II. Curvature, dispersion waves, and meandering waves. Physica D 46:416-426.

[28]Zykov, V.S. 1987a. Excitable media and autowave processes. In Simulation of wave processes in excitable media, edited by A. T. Winfree. Manchester, UK: Manchester University Press.

[29] Thakor, N.V., Jose M.F, J., Saiz, J., Grammatikov, B.I., and Jose M.F., Sr. 1998. Electrophysiologic models of heart cells and cell networks. Engineering in Medicine and Biology Magazine 17 (5):73-83.

[30] Zykov, V.S. 1987c. Simulation of the processes of circulation of an excitation in heart muscle. In Simulation of wave processes in excitable media, edited by A. T. Winfree. Manchester, UK: Manchester University Press.

[32] Williams, D., Thompson, D.G., Heggie, L., and Bancewicz, J. 1993, Resposes of the human esophagus to experimental intraluminal distension. American Journal of Physiology, 265 (Gastrointest. Liver Physiol.):G196-203

[31] Orvar, K.B., Gregerse, H., and Christensen, J.. 1993. Biomechanical characteristics of the human esophagus. Digestive Diseases Sciences 38:197-205.

[33] Kendall, G.P., Thompson, D.G., Day, S.J., and Garvie, N. 1987. Motor responses of the oesophagus to intraluminal distension in normal subjects and patients with oesophageal clearance disorders. Gut 28 (3):272-279.

[34] Diamant, N.E., 1989. Physiology of oesophageal motor function. Gastroenterology Clinics of North America 18 (2):179-194.

[35] MacDonald, N. 1989. How delays arise and what effects they have. In Biological delay systems: linear stability theory. Cambridge, UK: Cambridge University Press.

[36] Bell, G.H., Emslie-Smith, D., and Paterson, C.R. 1980. Neurone and Synapse. In BDS Textbook of Physiology. Edinburgh: Churchill Livingstone.

[37] Vales, P. 1976. A study of the arrangement and mechanical properties of the human descending colon of the large intestine. M.Sc., Department of Mechanical Engineering, University of Manchester Institute of Science and Technology, Manchester.

[38] Cotin, S., Delingette, H., and Ayache, N. 1999. Real-time elastic deformations of soft tissues for surgery simulation. IEEE Transactions on Visualization and Computer Graphics 5 (1):62-73.

[39] Pouderoux, P., Lin, S., and Kahrilas, P. 1997. Timing, propagation, coordination, and effect of esophageal shortening during peristalsis. Gastroenterology 112 (4):1147-1154.

Others

[40] AVS Express Visualization edition 3.0. 1996 Advanced Visual Systems Inc., Waltham, MA, USA.

[41] Miftakhov, R.N., and Wingate, D.L. 1995a. Mathematic modelling of the enteric nervous network. 5. Excitation propagation in a planar neural network. Medical Engineering and Physics 17 (1):11-9.

[42] Miftakhov, R.N., and Wingate, D.L. 1995b. Mathematical modelling of the enteric nervous network. 4. Analysis of adrenergic transmission. Medical Engineering and Physics 17 (1):3-10.